

Supporting Information

Simultaneously Enabling Superior ICE and High Rate/Cyclic Stability with Hollow Carbon Nanospheres anode for Sodium - Ion Storage

Dengke Liu,^a Yuqian Qiu,^a Yuxuan Du,^a Jiaying Yang,^a Xiaohan Jing,^a Xu Peng,^a Qiang Song,^{*} Fei Xu,^{*}

^a State Key Laboratory of Solidification Processing, Center for Nano Energy Materials, School of Materials Science and Engineering, Northwestern Polytechnical University and Shaanxi Joint Laboratory of Graphene (NPU), Xi'an, 710072, PR China.

* Corresponding author Email: songqiang511@nwpu.edu.cn; feixu@nwpu.edu.cn

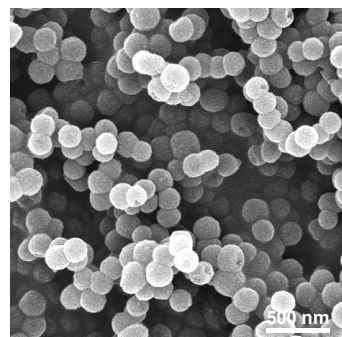


Figure S1. SEM images of PACP

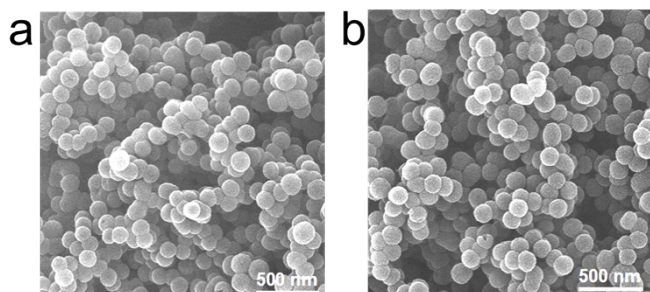


Figure S2. SEM images of (a) HCN-1100 and (b) HCN-1500.

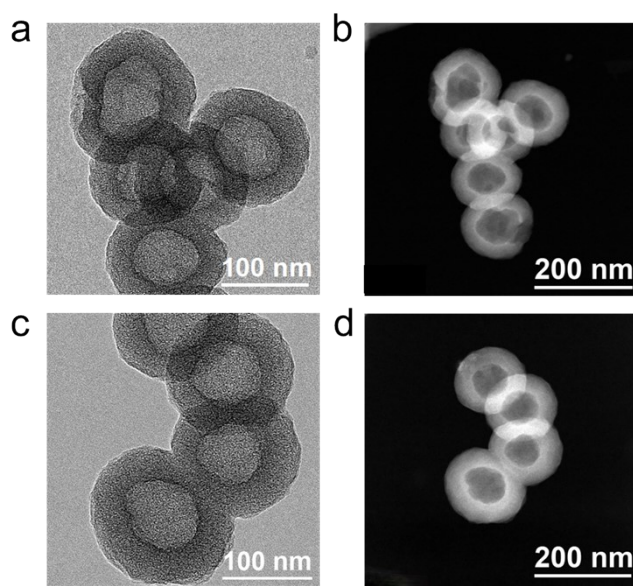


Figure S3. (a) TEM image of HCN-1100. (b) HAADF-STEM images of HCN-1100.
(c) TEM image of HCN-1500. (d) HAADF-STEM images of HCN-1500.

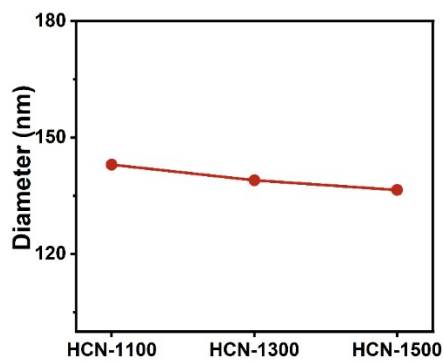


Figure S4. The diameter of HCNs.

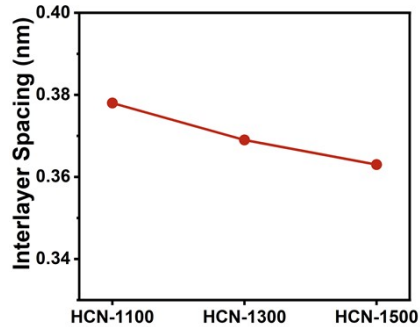


Figure S5. The interlayer spacing of HCNs from HRTEM.

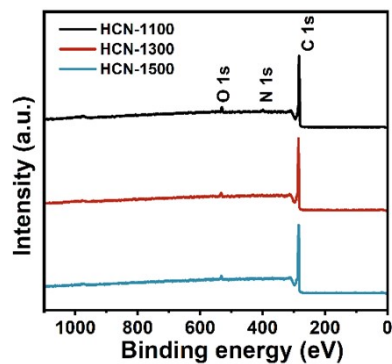


Figure S6. XPS Survey spectra of HCNs.

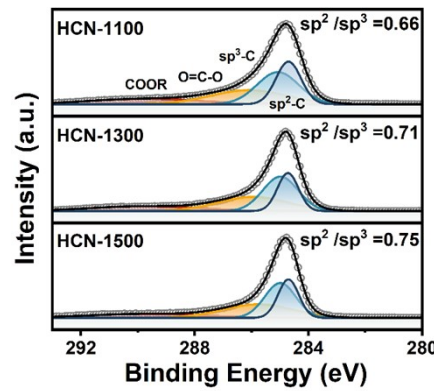


Figure S7. The fitting results of C 1s signals of HCNs.

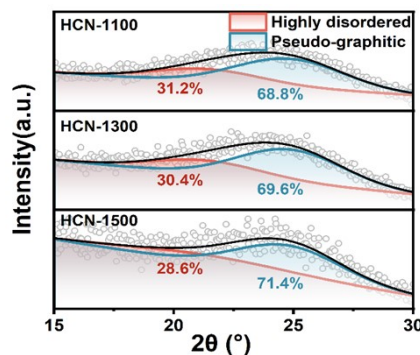


Figure S8. The (002) peak fitting of HCNs in XRD.

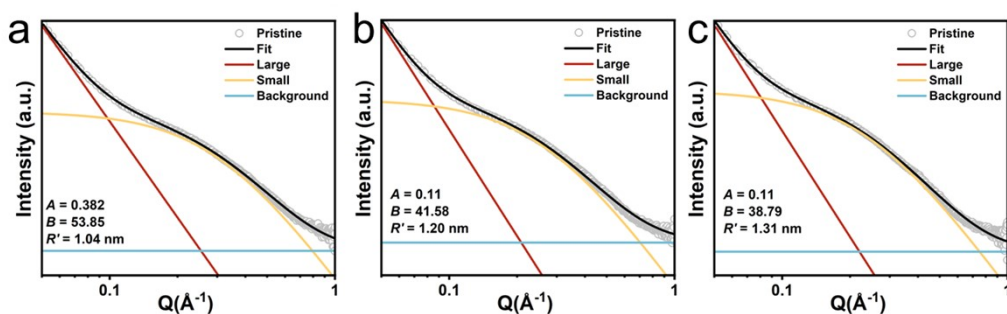


Figure S9. The fitted SAXS patterns of (a) HCN-1100, (b) HCN-1300 and (c) HCN-1500.

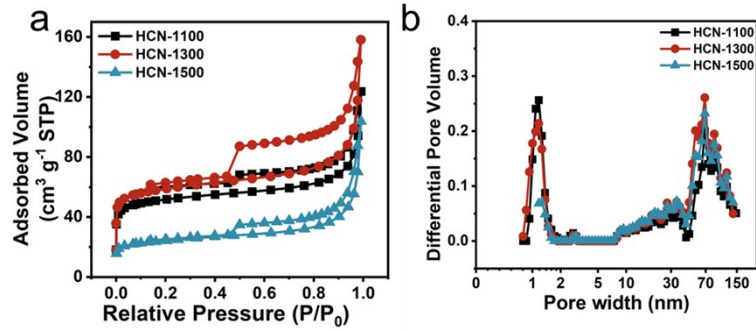


Figure S10. (a) N_2 adsorption-desorption isothermal curves of HCNs. (b) The pore size distribution of HCNs.

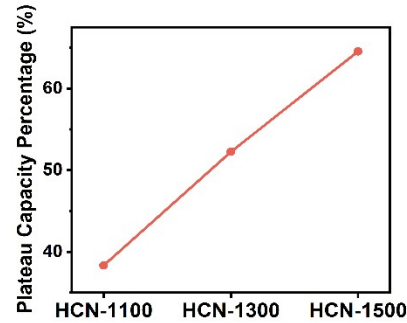


Figure S11. The linear correlation between carbonization temperature and plateau capacity.

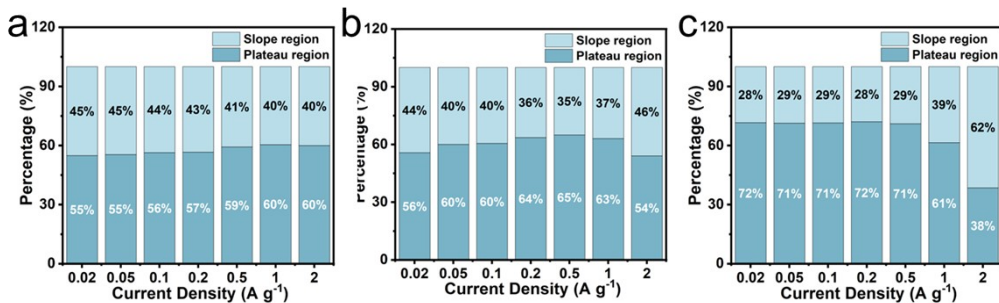


Figure S12. The capacity proportion of (a) HCN-1100, HCN-1300 (b) and (c) HCN-1500 at different current density.

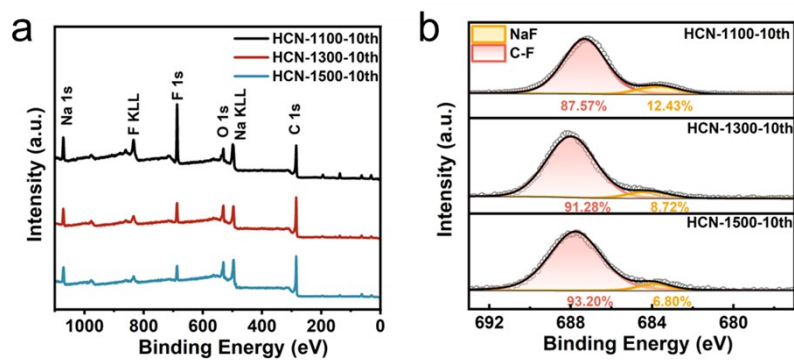


Figure S13. (a) XPS Survey spectra of HCNs after 10 cycles. (b) F 1s XPS spectra of HCNs after 10 cycles.

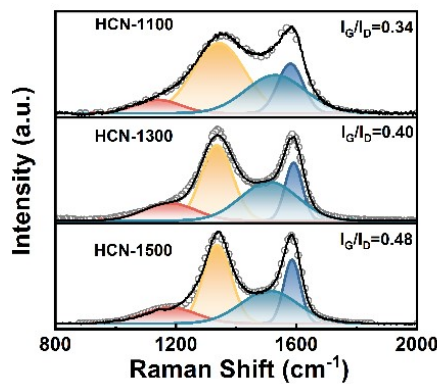


Figure S14. The Raman spectroscopy of HCNs after 10 cycles.

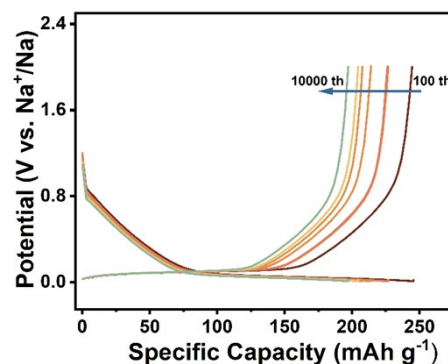


Figure S15. Galvanostatic charge/discharge curves for the different cycles at 1 A g⁻¹ of HCN-1300.

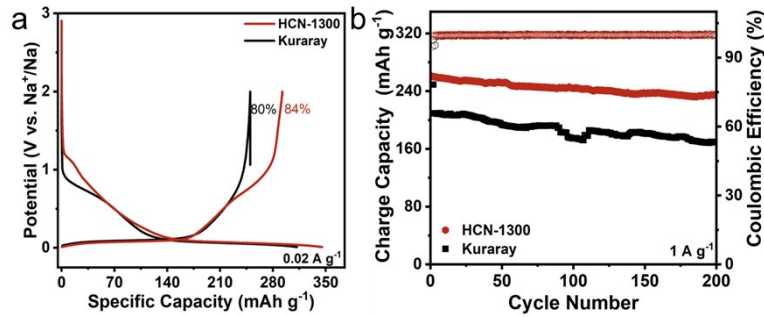


Figure S16. (a) Galvanostatic discharge/charge profiles of HCN-1300 and Kuraray at 0.02 A g^{-1} . (b) Cycle performance at 1 A g^{-1} of HCN-1300 and Kuraray.

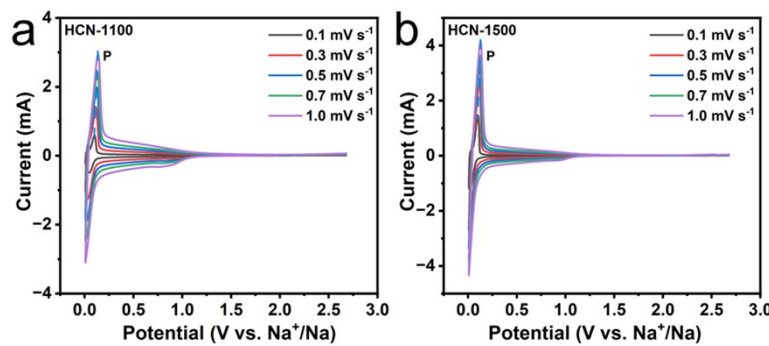


Figure S17. The CV curves of (a) HCN-1100 and (b) HCN-1500 at various scan rates.

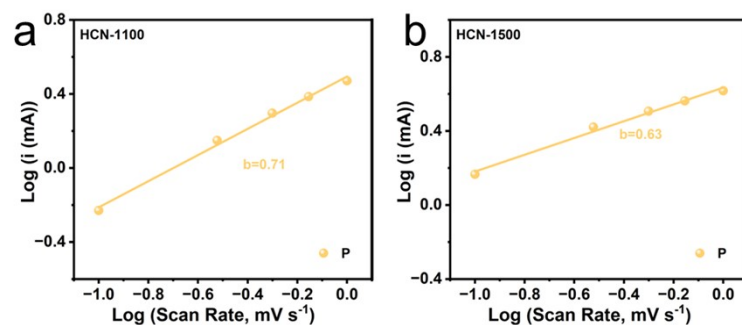


Figure S18. Relationship between peak currents and scan rates of (a) HCN-1100 and (b) HCN-1500.

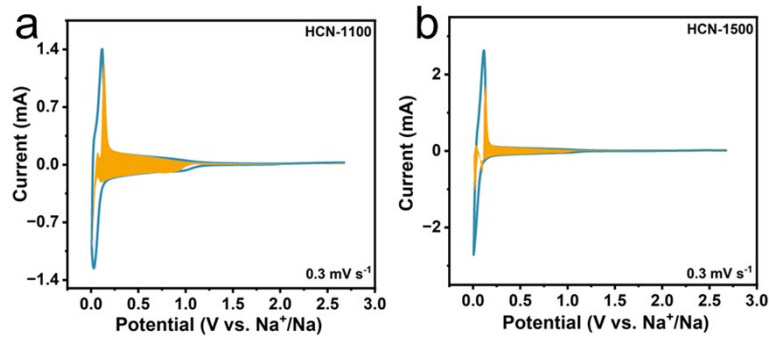


Figure S19. CV curve with a calculated capacitive contribution of (a) HCN-1100 and (b) HCN-1500 at 0.3 mV s^{-1} .

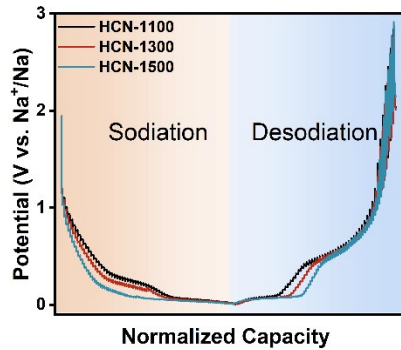


Figure S20. GITT potential profiles.

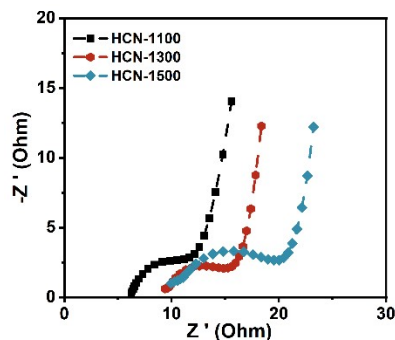


Figure S21. EIS measurements of HCNs.

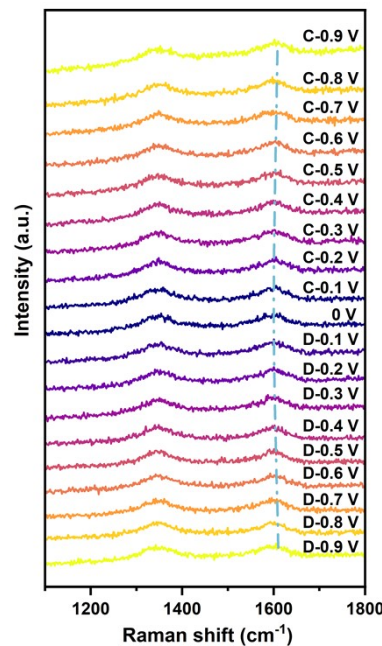


Figure S22. *In-situ* Raman spectra of HCN-1300, “C” stands for the charge state and “D” stands for the discharge state.

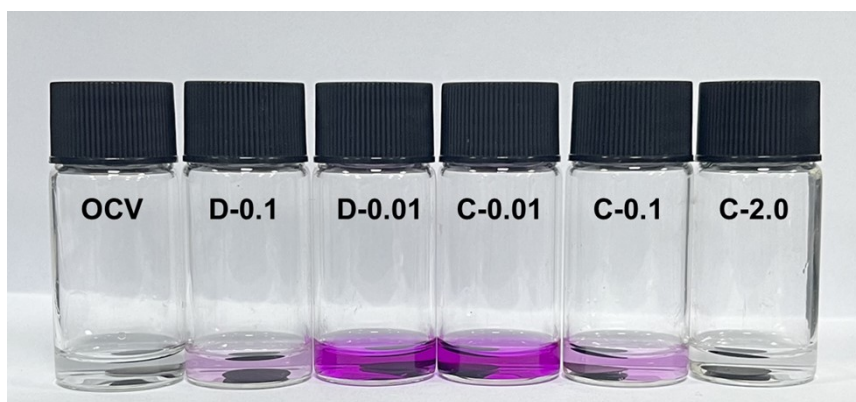


Figure S23. The color changes of ethanol containing 1% phenolphthalein after reaction with HCN-1300 at different potentials.

Table S1. Structure Parameters of HCNs.

Sample	I_G/I_D	L_a (nm)	d_{002} (nm)	L_c (nm)	$d_{closed\ pore}$ (nm)
HCN-1100	0.37	7.12	0.38	1.24	1.04
HCN-1300	0.44	8.51	0.37	1.36	1.21
HCN-1500	0.66	12.73	0.36	1.52	1.31

Table S2. Comparison of ICE performance hollow carbon nanospheres anodes.

Sample	ICE	Ref.
NNCS	20.47	S1
BFNHCS	24.7	S2
N-HCSs	30.28	S3
HCS	36	S4
DHCSs	37	S5
NCS	41.5	S6
3DHPCM-800	41.9	S7
PTA-NHCS-700	44.1	S8
N-DHCS	44.64	S9
HCF	47	S10
PCS	47.5	S11
P-HCS	56	S12
HCS-3	61.3	S13
4S-HCNs	72	S14
HTCS-900	80	S15
HCN-1300	84	This work

Table S3. Comparison of long cycling performance, ICE and rate performances with reported hard carbon materials.

Sample	ICE	Cycle	Rate performance		
			(Capacity/Current)	Ref.	HCN-1300 (This work)
LCS-73	82.9	1400	114 mAh g ⁻¹ (0.5 A g ⁻¹)	S16	261 mAh g ⁻¹ (0.5 A g ⁻¹)
FHC-1300	80	1000	107.1 mAh g ⁻¹ (2 A g ⁻¹)	S17	175 mAh g ⁻¹ (2 A g ⁻¹)
H-1500	~71	400	175 mAh g ⁻¹ (2 A g ⁻¹)	S18	175 mAh g ⁻¹ (2 A g ⁻¹)
HCK-1	80.4	600	138 mAh g ⁻¹ (2 A g ⁻¹)	S19	175 mAh g ⁻¹ (2 A g ⁻¹)
AMHC-900	76	2500	63 mAh g ⁻¹ (1 A g ⁻¹)	S20	230 mAh g ⁻¹ (1 A g ⁻¹)
SC-3	77	100	-	S21	-
CC-700	48	8000	120.6 mAh g ⁻¹ (1 A g ⁻¹)	S22	230 mAh g ⁻¹ (1 A g ⁻¹)
H300-1100	82.5	1000	60 mAh g ⁻¹ (1 A g ⁻¹)	S23	230 mAh g ⁻¹ (1 A g ⁻¹)
PNDCs-500CDs-1200°C	68.42	2500	~40 mAh g ⁻¹ (2 A g ⁻¹)	S24	175 mAh g ⁻¹ (2 A g ⁻¹)
POP3-1200	67.5	500	~85 mAh g ⁻¹ (0.6 A g ⁻¹)	S25	261 mAh g ⁻¹ (0.5 A g ⁻¹)
WNSC	83.1	800	~50 mAh g ⁻¹ (2 A g ⁻¹)	S26	175 mAh g ⁻¹ (2 A g ⁻¹)
Cel-O300-1500	74.8	50	~45.1 mAh g ⁻¹ (2 A g ⁻¹)	S27	175 mAh g ⁻¹ (2 A g ⁻¹)
CM-180	78.4	100	90.5 mAh g ⁻¹ (0.3 A g ⁻¹)	S28	261 mAh g ⁻¹ (0.5 A g ⁻¹)
MW-900	70.1	50	~83 mAh g ⁻¹ (0.5 A g ⁻¹)	S29	261 mAh g ⁻¹ (0.5 A g ⁻¹)
HCN-1300	84	10000	This work		

References

- S1 W. Zhang, C. Lan, X. Xie, Q. Cao, M. Zheng, H. Dong, H. Hu, Y. Xiao, Y. Liu and Y. Liang, *J. Colloid Interface Sci.*, 2019, **546**, 53-59.
- S2 X. Zhao, Y. Zhang, T. Liu, M. Xiao, B. Du, X. Lu, F. Zhu and Y. Meng, *J. Electroanal. Chem.*, 2023, **941**, 117553.
- S3 Y. Wen, B. Wang, B. Luo and L. Wang, *Eur. J. Inorg. Chem.*, 2016, **2016**, 2051-2055.
- S4 J. Ye, J. Zang, Z. Tian, M. Zheng and Q. Dong, *J. Mater. Chem. A*, 2016, **4**, 13223-13227.
- S5 L. Bu, X. Kuai, W. Zhu, X. Huang, K. Tian, H. Lu, J. Zhao and L. Gao, *Electrochim. Acta*, 2020, **356**, 136804.
- S6 K. Tang, L. Fu, R. J. White, L. Yu, M.-M. Titirici, M. Antonietti and J. Maier, *Adv. Energy Mater.*, 2012, **2**, 873-877.
- S7 G. Zou, H. Hou, X. Cao, P. Ge, G. Zhao, D. Yin and X. Ji, *J. Mater. Chem. A*, 2017, **5**, 23550-23558.
- S8 G. Huang, Q. Kong, J. Jiang, W. Yao and Q. Wang, *ChemSusChem*, 2022, **15**, e202201310.
- S9 K. Zhang, X. Li, J. Liang, Y. Zhu, L. Hu, Q. Cheng, C. Guo, N. Lin and Y. Qian, *Electrochim. Acta*, 2015, **155**, 174-182.
- S10 S. Feng, K. Li, P. Hu, C. Cai, J. Liu, X. Li, L. Zhou, L. Mai, B.-L. Su and Y. Liu, *ACS Nano*, 2023, **17**, 23152-23159.
- S11 D. Cheng, Z. Li, M. Zhang, Z. Duan, J. Wang and C. Wang, *ACS Nano*, 2023, **17**, 19063-19075.
- S12 L. Liu, Q. Li, Z. Wang and Y. Chen, *Mater. Technol.*, 2018, **33**, 748-753.
- S13 X. Chen, Y. Fang, H. Lu, H. Li, X. Feng, W. Chen, X. Ai, H. Yang and Y. Cao, *Small*, 2021, **17**, 2102248.
- S14 D.-S. Bin, Y. Li, Y.-G. Sun, S.-Y. Duan, Y. Lu, J. Ma, A.-M. Cao, Y.-S. Hu and L.-J. Wan, *Adv. Energy Mater.*, 2018, **8**, 1800855.
- S15 W. Zhong, D. Cheng, M. Zhang, H. Zuo, L. Miao, Z. Li, G. Qiu, A. Cheng and H. Zhang, *Carbon*, 2022, **198**, 278-288.
- S16 H. Chen, N. Sun, Q. Zhu, R. A. Soomro and B. Xu, *Adv. Sci.*, 2022, **9**, 2200023.
- S17 Z. Hou, D. Lei, M. Jiang, Y. Gao, X. Zhang, Y. Zhang and J.-G. Wang, *ACS Appl. Mater. Interfaces*, 2023, **15**, 1367-1375.
- S18 Z. Tang, R. Zhang, H. Wang, S. Zhou, Z. Pan, Y. Huang, D. Sun, Y. Tang, X. Ji, K. Amine and M. Shao, *Nat. Commun.*, 2023, **14**, 6024.
- S19 Z. Hou, M. Jiang, D. Lei, X. Zhang, Y. Gao and J.-G. Wang, *Nano Res.*, 2024, **17**, 5188-5196.
- S20 A. Patel, R. Mishra, R. K. Tiwari, A. Tiwari, D. Meghnani, S. K. Singh and R. K. Singh, *J. Energy Storage*, 2023, **72**, 108424.
- S21 Q. Li, X. Liu, Y. Tao, J. Huang, J. Zhang, C. Yang, Y. Zhang, S. Zhang, Y. Jia, Q. Lin, Y. Xiang, J. Cheng, W. Lv, F. Kang, Y. Yang and Q.-H. Yang, *Natl. Sci. Rev.*, 2022, **9**, nwac084.
- S22 R. Hao, Y. Yang, H. Wang, B. Jia, G. Ma, D. Yu, L. Guo and S. Yang, *Nano Energy*, 2018, **45**, 220-228.
- S23 M. Song, Z. Yi, R. Xu, J. Chen, J. Cheng, Z. Wang, Q. Liu, Q. Guo, L. Xie and C. Chen, *Energy Storage Mater.*, 2022, **51**, 620-629.
- S24 Y. Huang, X. Zhong, X. Hu, Y. Li, K. Wang, H. Tu, W. Deng, G. Zou, H. Hou and X. Ji, *Adv. Funct. Mater.*, 2024, **34**, 2308392.

- S25 L. Ji, Y. Zhao, L. Cao, Y. Li, C. Ma, X. Qi and Z. Shao, *J. Mater. Chem. A*, 2023, **11**, 26727-26741.
- S26 L. Shang, R. Yuan, H. Liu, X. Li, B. Zhao, X. Liu, A. Li, X. Chen and H. Song, *Carbon*, 2024, **223**, 119038.
- S27 B. Zhao, X. Li, L. Shang, C. Qiu, R. Yuan, H. Liu, T. Liu, A. Li, X. Chen and H. Song, *J. Mater. Chem. A*, 2024, **12**, 5834-5845.
- S28 S. Zhang, N. Sun, M. Jiang, R. A. Soomro and B. Xu, *Carbon*, 2023, **209**, 118034.
- S29 P. Zhang, Y. Shu, Y. Wang, J. Ye and L. Yang, *J. Mater. Chem. A*, 2023, **11**, 2920-2932.